JOURNAL OF MATERIALS SCIENCE 29 (1994) 894–898

Initiation of recrystallized grain structure under high-temperature low-cycle fatigue in 304 stainless steel

H. IIZUKA
Department of Mechanical Engineering, Yamagata University, Jonan 4-3-16, Yonezawa 992, Japan

N. SATO
Chita Works, Kawasaki Steel Corp., 1-1 Kawasaki cho, Handa 475, Japan

Initiation of recrystallized grains was observed under high-temperature low-cycle fatigue conditions in austenitic 18Cr–8Ni stainless steel. The fatigue tests were carried out using unbalanced fast-tension and slow-compression triangular strain wave-shape at 973 K in air. Recrystallized grains were initiated and grew along grain boundaries with the number of fatigue cycles. Accumulated grain-boundary sliding is considered to be the driving force for the recrystallization. Effects of the recrystallized grain structure on high-temperature fatigue failure were then examined under the conditions in which intergranular fatigue failure occurred. The recrystallized grain structure had no detrimental effects on the intergranular failure. The fatigue life was somewhat increased by the initiation of recrystallized grain structure.

1. Introduction

In high-temperature low-cycle fatigue conditions, the extent of accumulated fatigue damage is difficult to estimate, because two modes of inelastic strains (creep and plasticity) may exist separately or concurrently. The strain-range partitioning approach [1] is a useful method for estimating accumulated fatigue damage. The effects of wave shape and testing temperatures were discussed using this approach. Moreover, recent measurements of grain-boundary sliding (GBS) indicate the importance of GBS in high-temperature intergranular fatigue-failure [2–6]. Namely, the occurrence of GBS and subsequent crack initiation are important processes of fatigue-damage accumulation. Kitagawa [2] measured the amount of GBS under torsional reversed creep and fatigue loading in lead. McLean and Pineau [6] explained the effect of hold-time on fatigue life in terms of damage produced by GBS. Further, Taira *et al.* [4] studied the effects of wave shapes on GBS accumulation. GBS rate was high under asymmetrical wave-shape cyclings, such as unbalanced slow–fast or fast–slow triangular wave shapes [4]. We have investigated previously [5] the effects of grain size on GBS rate and on wedge-type crack initiation by GBS.

Metallurgical behaviour such as recrystallization and grain-boundary migration during high-temperature deformation is another important process associated with fatigue-damage accumulation. Grain-boundary migration was investigated during cycling using aluminium alloys [7], α-iron [8], copper and 304 stainless steel [9], or during creep [10]. Recrystallization is well accepted during creep or constant strain-rate deformation at high temperature [10]. This metallurgical behaviour may affect creep-fatigue interaction, because the metallurgical changes are diffusion-controlled processes and they become increasingly important at elevated temperature. Moreover, these studies are useful in understanding what microstructural features contribute to superior high-temperature fatigue resistance. However, the effects of recrystallization on fatigue properties have not been sufficiently studied.

In this work, initiation and growth of recrystallized grain structure under high-temperature low-cycle fatigue were observed in 18Cr–8Ni stainless steel at 973 K in air. The effects of recrystallized grain structure on fatigue failure were then studied under conditions in which intergranular failure occurred. The effects of general grain size on recrystallization were also examined.

2. Experimental procedure

The material used was austenitic 18Cr–8Ni stainless-steel. The basic chemical compositions were 18.24% Cr, 8.72% Ni, 0.072% C, 1.19% Mn, 0.34% Si (by weight), balance iron. The solution heat treatments performed were water quenching after 0.5 h holding at 1323 K, 0.5 h holding at 1423 K and 5 h holding at 1573 K. The general grain diameters, D, obtained were about 40, 130 and 400 μm, respectively. Hourglass-shaped testpieces with smooth surfaces were machined from these heat-treated materials. The testpiece diameter of the gauge portion was 6 mm and the gauge

0022–2461

length was 12 mm. The testpieces had two circular ridges for mounting of extensometers at either end of the gauge length. Measurement and control of axial strain was approached through the ridges.

High-temperature low-cycle fatigue tests were carried out using servo-controlled fatigue-test equipment at 973 K in air. We investigated creep-fatigue interaction, and observed the initiation of recrystallized grain structure in tests with fast-tension and slow-compression (fast–slow) unbalanced triangular strain wave shapes. Recrystallized grain structure was not observed in tests with fast–fast, slow–fast and slow–slow wave shapes. Therefore, the experiments on recrystallization were carried out using fast–slow strain wave shape. Fig. 1a shows the fast–slow wave shape. The nominal strain rate among the gauge lengths for fast tension, $\dot{\varepsilon}_{fast}$, was 1.0×10^{-2} s^{-1}, and for slow-compression, $\dot{\varepsilon}_{slow}$, was 1.0×10^{-5} s^{-1}. The total strain range, $\Delta\varepsilon_T$, was 1.0%. The tests were periodically stopped every 100–110 fatigue cycles and cooled to room temperature to observe microstructure. Recrystallized grain structure was observed using an optical microscope of 400–1000 magnification after electrolytic corrosion. Grain-boundary sliding (GBS) which accumulated during a given fatigue cycling was measured using a scanning electron microscope of 3000–10 000 magnification.

In order to study the influence of recrystallized grain structure on fatigue failure, fatigue life tests were carried out using testpieces with recrystallized grain structure, which was produced by the fast–slow wave-shape cyclings. The wave shape used in the fatigue-life tests was slow–fast unbalanced strain wave shape, under which intergranular fatigue failure occurred. Fig. 1b shows the slow–fast wave shape. $\dot{\varepsilon}_{slow}$ was 1.0×10^{-5} s^{-1}, $\dot{\varepsilon}_{fast}$ was 1.0×10^{-2} s^{-1}, and $\Delta\varepsilon_T$ was 1.0%. Fatigue cracks and fracture surfaces were observed by using optical and scanning electron microscopy.

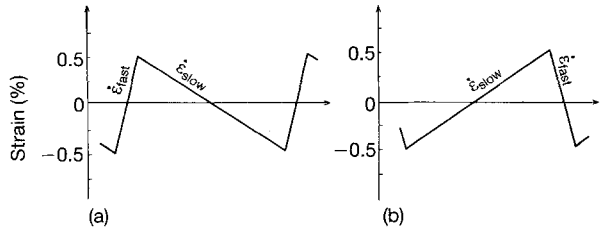

Figure 1 Fatigue wave shapes: (a) fast–slow, (b) slow–fast.

3. Results and discussion

3.1. Initiation and growth of recrystallized grain structure

Fig. 2 shows recrystallized grain structure initiated in $D = 40$ μm testpieces. N_1 is the number of fast–slow fatigue cycles performed to produce recrystallized grain structure. The recrystallized grains were produced initially at grain-boundary triple junctions and grain-boundary ridges, and then grew along grain boundaries with the number of fatigue cycles. Many recrystallized grains were observed after $N_1 = 200$ cycles. Fig. 3 shows the microstructure of $D = 130$ and 400 μm testpieces. The recrystallized grain diameter was about 3–5 μm, and was much the same in $D = 40$, 130 and 400 μm testpieces. The extent of recrystallization was large in the testpieces with small D. The tendency may be explained by dislocation density, which is high in testpieces with small D [11].

The stored energy by cyclic plastic deformation is considered to be the driving force for recrystallization. Fig. 4 shows a scanning electron micrograph of a plastic replica that was obtained from the surface of a $D = 130$ μm testpiece. The loading direction was longitudinal in the micrograph. The marker lines parallel to the loading axis were produced on the testpiece surface by placing sand paper on it and drawing this over the surface. According to the strain-range partitioning approach [1], there were two types of inelastic

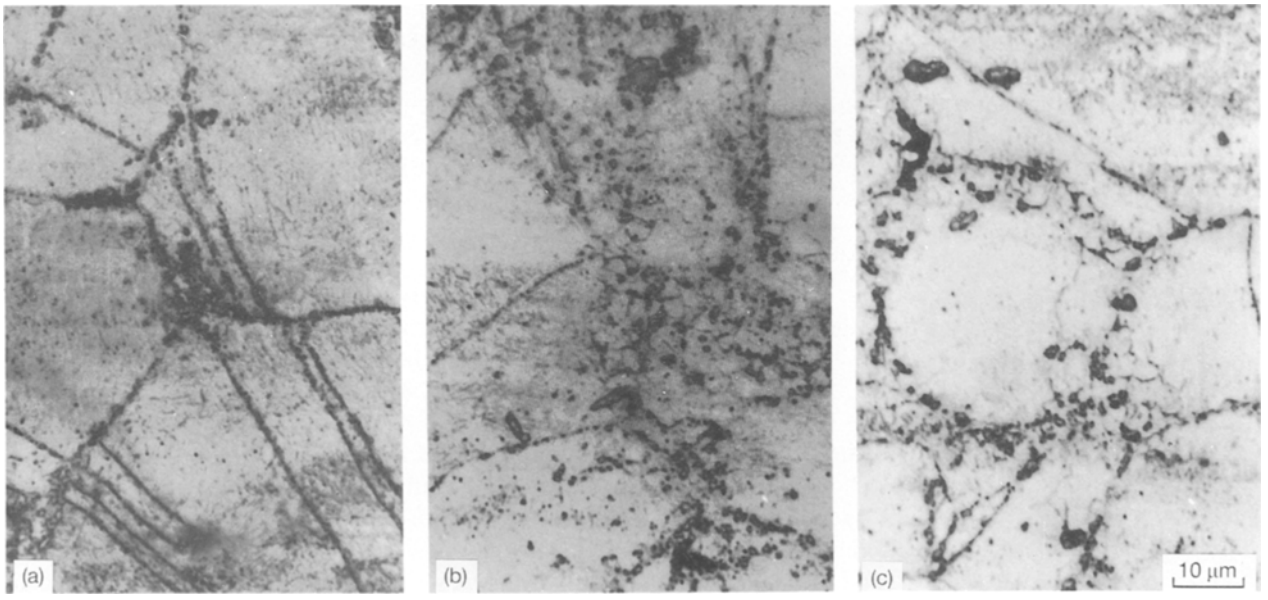

Figure 2 Recrystallized grain structure observed in $D = 40$ μm testpieces at (a) $N_1 = 100$ cycles, (b) $N_1 = 200$ cycles and (c) $N_1 = 308$ cycles.

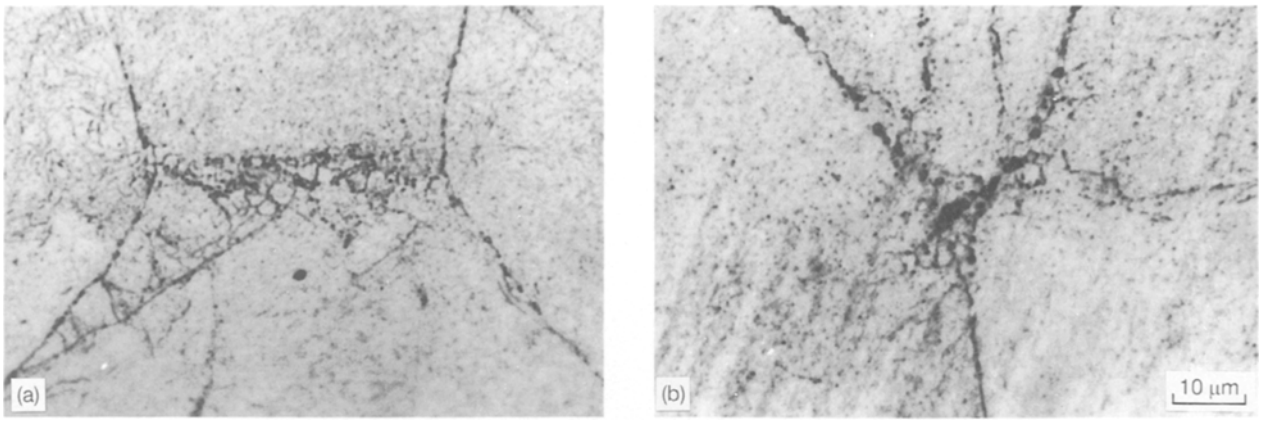

Figure 3 Recrystallized grain structure observed in (a) $D = 130$ μm testpieces at $N_1 = 321$ cycles and (b) $D = 400$ μm testpieces at $N_1 = 315$ cycles.

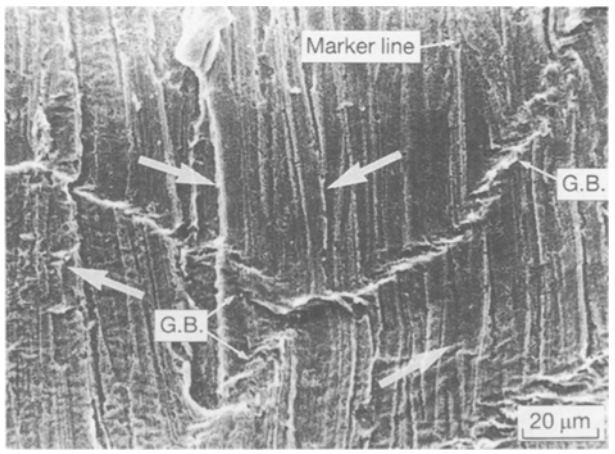

Figure 4 Scanning electron micrograph of a plastic replica, showing grain-boundary sliding which occurred in a $D = 130$ μm testpiece at $N = 196$ cycles.

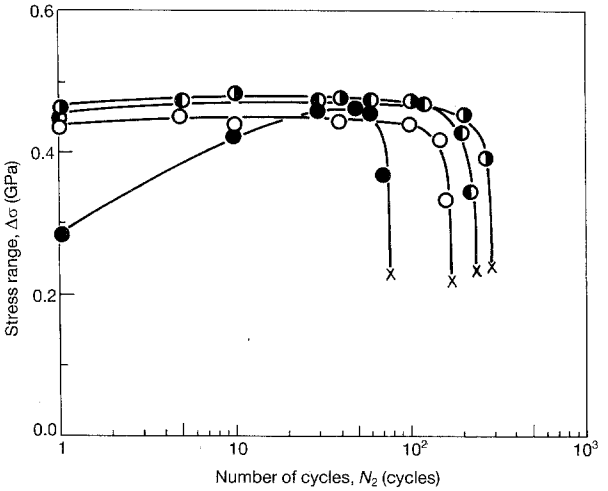

Figure 5 Effects of recrystallized grain structure on cyclic stress range in $D = 40$ μm testpieces; $\Delta\varepsilon_T = 1.0\%$. N_1: (●) 0 cycle, (○) 100 cycles, (○) 200 cycles, (○) 315cycles.

strain ranges in the fast–slow fatigue cyclings, namely tensile plastic reversed by compressive creep strain range, $\Delta\varepsilon_{pc}$, and tensile plastic reversed by compressive plastic strain range, $\Delta\varepsilon_{pp}$. $\Delta\varepsilon_{pc}$ was about 0.60% in this case. It is known that GBS occurs during the creep portions where strain rate was low [4]. Therefore, GBS is accumulated in one direction with the fast–slow fatigue cyclings. Arrows in Fig. 4 indicate the direction. The maximum amount of accumulated GBS was about 9 μm along the grain boundary shown in Fig. 4. The value was extremely large compared with the critical amount of GBS for wedge-type crack initiation, which was of the order of 0.1 μm under high-temperature low-cycle fatigue with slow–fast and slow–slow triangular wave shapes [5]. The large amount of stored energy was not released by wedge-type crack initiation.

3.2. Effects of recrystallized grain structure on fatigue failure

The influences of grain-boundary microstructure are more important under the fatigue conditions in which cracks propagate along grain boundaries. Therefore, the effects of recrystallized grain structure on fatigue failure were examined in tests with an unbalanced slow–fast wave shape. It is well known that the fatigue cracks propagate along grain boundaries in fatigue tests with slow–fast wave shapes [1].

Fig. 5 shows the stress range, $\Delta\sigma$, during the failure tests. The life of N_2 was longer in testpieces with recrystallized grains ($N_1 > 0$) than in that with no recrystallized grains ($N_1 = 0$). The maximum stress range was almost equal to that of the testpieces with no recrystallized grain structure, though work hardening was not observed in the testpieces with recrystallized grains. The work hardening was already saturated during the fast–slow wave shape cyclings. Moreover, inelastic strain ranges, $\Delta\varepsilon_{in}$, at about half-life cycle ($N_2/2$) were also almost equal in all the testpieces. Namely, $\Delta\varepsilon_{in}$ was about 0.75, 0.75, 0.75 and 0.70 in testpieces with $N_1 = 0$, 100, 200 and 315 cycles, respectively. The results indicate that the influence of the recrystallized grain structure on the cyclic deformation was small. Therefore, the increase of fatigue life of N_2 is not reduced to the change of cyclic deformation.

Fig. 6 shows the relationship between fatigue life (N_2/N_{fcp}) observed in slow–fast tests and fatigue precycles (N_1/N_{fpc}) that was performed for the production

of recrystallized grains. N_{fcp} is cyclic life for partitioned strain range of $\Delta\varepsilon_{cp}$ [1]. N_{fpc} is that for $\Delta\varepsilon_{pc}$. N_{fcp} = 100, 85 and 75 cycles, and N_{fpc} = 850, 820 and 800 cycles for D = 40, 130 and 400 μm testpieces, respectively. N_2/N_{fcp} was higher in the testpieces with recrystallized grain structure than in that with no recrystallized grain structure. N_2/N_{fcp} increased with increasing N_1/N_{fpc} up to about N_1/N_{fpc} = 0.3. The largest value of N_2/N_{fcp} was 2.8. Moreover, N_2/N_{fcp} was highest in D = 40 μm testpieces where a large amount of recrystallized grains was produced, as shown in Fig. 1. N_2/N_{fcp} then decreased with the number of fatigue cycles of N_1/N_{fpc} after the maximum values. The decrease was explained by the influence of fatigue cracks that were initiated during the fast–slow pre-cycling.

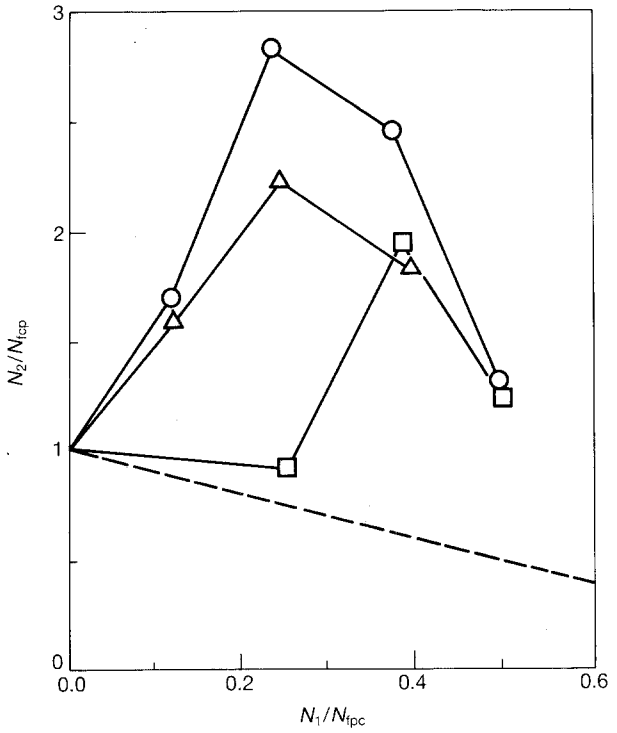

Figure 6 Relationship between fast–slow fatigue life, N_1/N_{fpc}, and slow–fast fatigue life, N_2/N_{fcp}. D: (○) 40 μm, (△) 130 μm, (□) 400 μm.

The broken line in Fig. 6 shows the linear damage summation rule [9], i.e.

$$\sum(N_k/N_{fij}) = C \quad (1)$$

where N_k is N_1 and N_2, N_{fij} is N_{fpc} and N_{fcp}. Fatigue failure occurs when total damage, C, is equal to unity. However, it has been found that the linear damage summation rule is not applicable when different kinds of damage are accumulated in series [8]. The data in Fig. 6 also indicates that the constant C is not unity. It is considered that the initiation of recrystallization is one reason for this. Moreover, C is larger than unity. The recrystallized grain structure has a strengthening effect on intergranular fatigue-crack initiation or propagation resistance.

3.3. Microstructural observations of failed testpieces

Fig. 7 shows the fracture surfaces of D = 130 μm testpieces. Small irregularities were observed at the fracture surfaces. Arrows in Fig. 7 indicate the irregularities. The irregularities were increased with the number of fast–slow fatigue cycles (Fig. 7b). Fig. 8 shows the microcrack that initiated inside testpieces with D = 400 μm. The crack propagated along recrystallized grain boundaries. The micrograph indicates that the irregularities corresponded to the intergranular fracture surface of the recrystallized grains. Similar fracture surfaces were observed in D = 40 and 400 μm testpieces.

Fatigue cracks were also initiated at testpiece surfaces. Fig. 9 shows the surface cracks that were observed in D = 400 μm testpieces. The fatigue cracks were initiated in an oxide layer [12] that was produced along grain boundaries. This kind of crack initiation was also observed in D = 40 and 130 μm testpieces. The surface-crack initiation-life was 30–40 cycles. In the testpieces with no recrystallized grain structure, wedge-type cracks were initiated by GBS at the testpiece surface. We have confirmed [5] that the wedge-type crack initiation life was less than 5 cycles under the same fatigue conditions. The results show that the initiation of wedge-type crack was inhibited

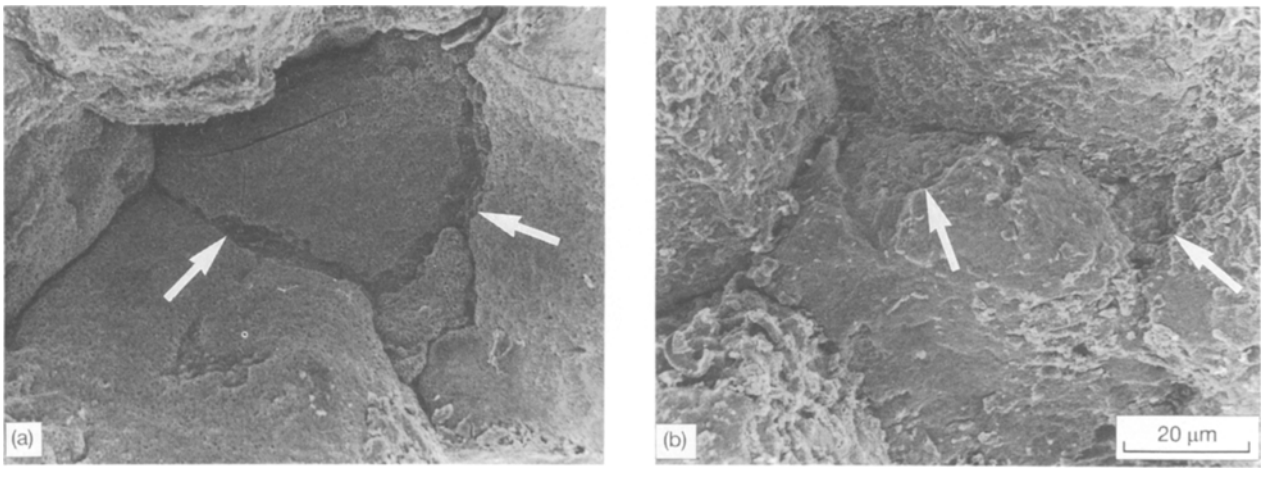

Figure 7 Fracture surfaces of D = 130 μm testpieces in testpieces with (a) N_1 = 100 cycles and (b) N_1 = 200 cycles.

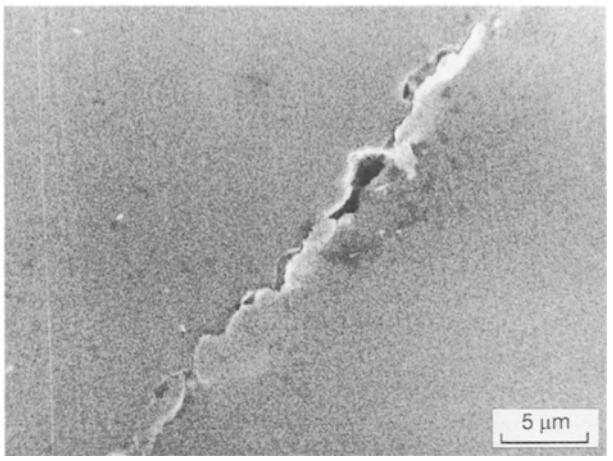

Figure 8 Internal fatigue cracks observed in $D = 400\ \mu m$ failed testpiece; $N_1 = 315$ cycles and $N_2 = 93$ cycles.

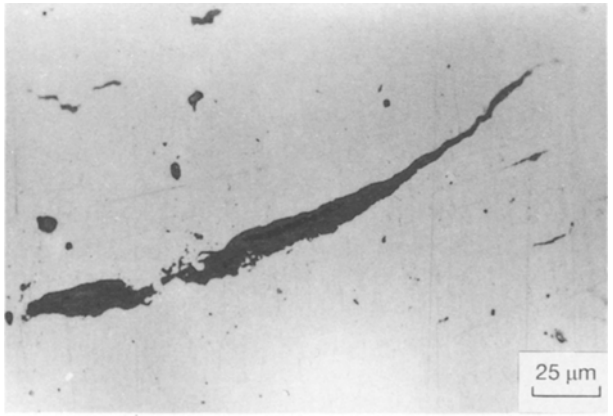

Figure 9 Surface fatigue crack observed in $D = 130\ \mu m$ failed testpiece; $N_1 = 321$ cycles and $N_2 = 150$ cycles.

by the recrystallized grain structure. The strengthening mechanism may be identical with that of "necklace" microstructure [13–16], which has a very interesting compromise of good creep resistance of large general grains and resistance to low-cycle fatigue by fine recrystallized grains.

4. Conclusions

Recrystallization during fast–slow fatigue cycling at high temperature was observed in austenitic 18Cr–8Ni stainless steel at 973 K in air. The effects of recrystallized grains on fatigue failure were then examined under fatigue where intergranular failure occurred. The results obtained can be summarized as follows.

1. Recrystallized grains were initiated and grew along grain boundaries in fatigue with fast–slow triangular wave shape. In this wave-shape test, a large amount of grain-boundary sliding that took place during slow-compressive loading was accumulated along the grain boundaries.

2. Recrystallized grain structure had no detrimental effects on intergranular fatigue failure. Fatigue life was somewhat increased by the existence of recrystallized grain structure. The longest life was 2.8 times compared with that in testpieces with no recrystallized grain structure.

3. Surface cracks were initiated in oxide layers that were produced along grain boundaries. The surface crack initiation life was increased by the existence of recrystallized grain structure. Fatigue cracks were also initiated inside testpieces, and propagated along recrystallized grain boundaries.

Acknowledgement

The authors thank Dr M. Tanaka, Associate Professor, Akita University, for his valuable advice during the course of this study.

References

1. S. S. MANSON, ASTM STP 520 (American Society for Testing and Materials, Philadelphia, PA, 1973) p. 744.
2. M. KITAGAWA, ASTM STP 519 (American Society for Testing and Materials, Philadelphia, PA, 1973) p. 58.
3. K. U. SNOEDEN, in "Cavities and Cracks in Creep and Fatigue", edited by J. Gittus (Applied Science, London, 1981) p. 259.
4. S. TAIRA, M. FUJINO and M. YOSHIDA, *J. Soc. Mater. Sci. Jpn* **27** (1978) 447 (in Japanese).
5. H. IIZUKA and M. TANAKA, *Mater. High Temp.* **9**(1) (1991) 17.
6. D. McLEAN and A. PINEAU, *Metal Sci.* **12** (1978) 313.
7. T. G. LANGDON and V. RAMAN, in "Grain Boundary Structure and Related Phenomena", edited by Y. Ishida *et al.* (Japan Institute of Metals, Sendai, 1986) p. 747.
8. H. J. WESTWOOD and D. M. R. TAPLIN, *Metall. Trans.* **3** (1972) 1959.
9. H. A. RAOUF, A. PLUMTREE and T. H. TOPPER, *Metall. Trans.* **5** (1974) 267.
10. J. P. POIRIER, "Creep of Crystals" (Cambridge University Press, Cambridge, 1985) p. 179.
11. J. G. BYNE, in "Recovery Recrystallization and Grain Growth" (Maruzen, Tokyo, 1968) p. 28.
12. T. KITAGAWA, N. TADA, M. ABE, M. YUMITA and R. OHTANI, *Trans. Jpn Soc. Mech. Eng.* **56** (1990) 575.
13. C. E. SHAMBLEN, R. E. ALLEN and F. E. WALKER, *Metall. Trans.* **6A** (1975) 2073.
14. A. PINEAU, in "Subcritical Crack Growth due to Fatigue, Stress Corrosion and Creep", edited by L. H. Larsson (Elesevier Applied Science, London, 1981) p. 483.
15. A. D. BOYD-LEE and J. E. KING, in "Proceedings of Fatigue" (Hawaii, Materials and Components Engineering Publications Ltd, Birmingham, 1990) p. 1205.
16. M. JEANDIN, *J. Mater. Sci.* **17** (1982) 2902.

Received 12 October 1992
and accepted 24 August 1993